JACS
JOURNAL OF THE AMERICAN CHEMICAL SOCIETY
Article
pubs.acs.org/JACS

Reductive Cleavage of CO_2 by Metal−Ligand-Cooperation Mediated by an Iridium Pincer Complex

Moran Feller,*[,†] Urs Gellrich,[†] Aviel Anaby,[†] Yael Diskin-Posner,[‡] and David Milstein*[,†]

Departments of [†]Organic Chemistry and [‡]Chemical Research Support, Weizmann Institute of Science, Rehovot 76100, Israel

Supporting Information

ABSTRACT: A unique mode of stoichiometric CO_2 activation and reductive splitting based on metal−ligand-cooperation is described. The novel Ir hydride complexes [(^{t}Bu-PNP*)Ir(H)$_2$] (**2**) (^{t}Bu-PNP*, deprotonated ^{t}Bu-PNP ligand) and [(^{t}Bu-PNP)Ir(H)] (**3**) react with CO_2 to give the dearomatized complex [(^{t}Bu-PNP*)Ir-(CO)] (**4**) and water. Mechanistic studies have identified an adduct in which CO_2 is bound to the ligand and metal, [(^{t}Bu-PNP-COO)Ir(H)$_2$] (**5**), and a di-CO_2 iridacycle [(^{t}Bu-PNP)Ir(H)(C_2O_4-$\kappa_{C,O}$)] (**6**). DFT calculations confirm the formation of **5** and **6** as reversibly formed side products, and suggest an η^1-CO_2 intermediate leading to the thermodynamic product **4**. The calculations support a metal−ligand-cooperation pathway in which an internal deprotonation of the benzylic position by the η^1-CO_2 ligand leads to a carboxylate intermediate, which further reacts with the hydride ligand to give complex **4** and water.

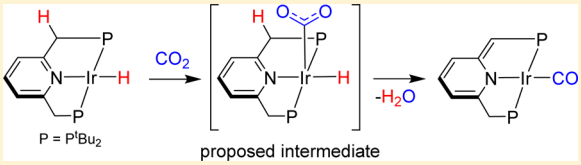

INTRODUCTION

The fundamental reactivity patterns of CO_2 with transition metal complexes are of much current interest.[1] CO_2 binding to metal centers is versatile and can involve metal−carbon σ bonding (η^1−C) or metal−oxygen bonding (η^1−O, η^2−O,O) and π bonding (η^2−CO).[1g] CO_2 can also serve as a bridging ligand, forming polymetallic complexes.[2] The Lewis acidic carbon atom and the Lewis basic oxygen atoms of CO_2 allow its bifunctional activation by early late bimetallic complexes, as was described for the dimer Ir−(μ^2−$\eta^2_{C,O}$)−CO_2−Zr.[3] CO_2 coordination was reported for complexes with a pendant Lewis basic ligand, which binds to the carbon atom of CO_2 while the oxygen atom is bound to the metal center, as in frustrated Lewis pairs.[4] Bifunctional CO_2 activation, where the CO_2 carbon atom acts as an electrophile on an activated site of a ligand was reported for PMI−Mo (PMI, pyridine monoamine),[5] β-diketiminate Sc,[6] and Pd diphenylphosphinoacetate complexes.[7] Reductive coupling of two CO_2 molecules to give a stable metallacycle was reported for Ir[8] and Rh[9] complexes, and it is assumed to be formed by nucleophilic attack of the oxygen atom in bound η^1−CO_2 on a free CO_2 molecule. Reductive coupling of CO_2 to give oxalate is also known.[10]

Another mode of CO_2 activation is CO_2 insertion into a metal−ligand bond, such as insertion into metal−alkyl,[11] aryl[11b,12] and allyl[11d,13] bonds. CO_2 insertion into metal−hydroxide[14] and alkoxide[14b,g,15] bonds leads to carbonate complexes, while CO_2 insertion into a metal−amide bond leads to carbamates.[14b,16,17] CO_2 insertion into a metal−hydride bond yields a formato complex,[18,10a,19] a key step in catalytic CO_2 hydrogenation to formic acid and formate salts.[20] The most efficient metal complex catalyst for the hydrogenation of CO_2 to formate by H_2 is the Ir(III) ^{i}Pr-PNP complex reported by Nozaki and co-workers.[21]

CO_2 reduction to CO by metals can take place by several different pathways: reductive cleavage of CO_2 to CO and water (reverse water gas shift reaction),[22] reductive disproportionation by oxide transfer from metal−η^1−CO_2 to free CO_2 affording M−CO and CO_3^{-2},[23] or oxygen transfer from CO_2 to an oxygen acceptor such as hydride and phosphine ligands or an oxophilic metal.[23c,24] Kaska, Mayer, Harrison, and co-workers reported the reaction of Ir an Rh hydride complexes with CO_2 to give formate complexes as intermediates, which disproportionate to carbonyl complexes.[18,19]

Recently, we reported a new binding mode of CO_2 promoted by metal−ligand-cooperation (MLC) by PNP dearomatized pincer complexes of Fe,[25] Ru,[26] and Re[27] (PNP, 2,6-bis(di*tert*-butylphosphinomethyl)pyridine). A concerted 1,3 addition of CO_2 by the metal center and the deprotonated benzylic position of the PNP ligand takes place to form new C−C and M−O bonds. Similar reactivity with PNN−Ru was reported by Sanford and co-workers.[28] Berke and co-workers demonstrated CO_2 activation by MLC with (PN^HP) Mo and W complexes (PN^HP, (^{i}Pr$_2$PCH$_2$CH$_2$)$_2$NH).[29]

Here, we present a novel mode of stoichiometric CO_2 reductive cleavage to CO and water by an Ir(I) hydrido pincer complex via MLC.[30] We have reported in the past MLC activation of H_2,[31] Csp^2−H[31], and Csp^3−H[32] bonds by Ir(I) ^{t}Bu-PNP complexes. Recently, we have reported the activation of O_2 by an Ir(I) ^{t}Bu-PNP complex, involving a MLC mechanism in which proton transfer from the benzylic position of the PNP ligand to a peroxo ligand took place, yielding a dearomatized hydroxo complex.[14a] Herein we suggest that proton transfer from the pincer ligand to an η^1−CO_2 adduct

Received: January 7, 2016
Published: April 28, 2016

DOI: 10.1021/jacs.6b00202
J. Am. Chem. Soc. 2016, 138, 6445−6454

can lead to CO_2 reductive cleavage, as evidenced experimentally and computationally.

RESULTS AND DISCUSSION

Synthesis and Characterization of [(^{t}Bu-PNP*)Ir(H)$_2$] and [(^{t}Bu-PNP)IrH]. Reaction of [(^{t}Bu-PNP)Ir(H)$_2$][PF$_6$] (**1**)[33] with 1 equiv of base (KHMDS in toluene or ^{t}BuOK in THF) resulted in the formation of a 3:7 mixture of [(^{t}Bu-PNP*)Ir(H)$_2$] (**2**) (^{t}Bu-PNP*, deprotonated ^{t}Bu-PNP ligand) and [(^{t}Bu-PNP)IrH] (**3**), respectively (Scheme 1). Upon addition of the base to complex **1** at 195 K, and following the reaction progress at low temperatures by NMR, it was observed that complex **2** is the kinetic product, while complex **3** was obtained at elevated temperatures (Figure 1). The ^{31}P{^{1}H}

Scheme 1. Deprotonation of Complex 1 To Give a Mixture of 2 and 3

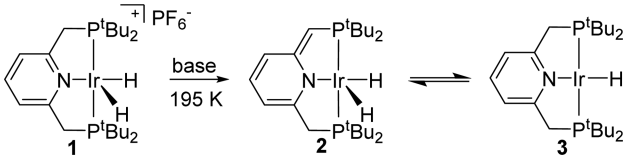

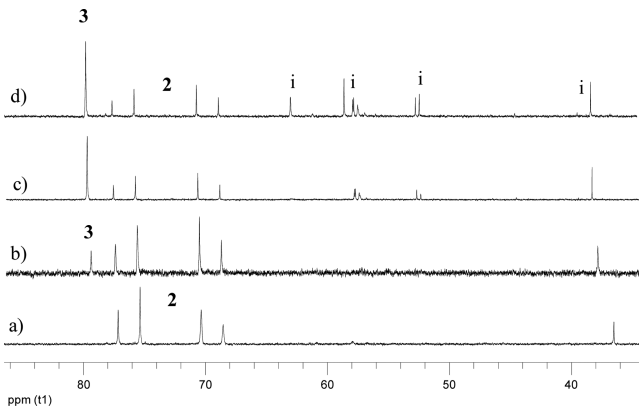

Figure 1. Variable temperature ^{31}P{^{1}H} NMR spectrum of the reaction mixture of **1** with KHMDS in toluene-d_8 to give **2** and **3**: (a) 230 K, (b) after 30 min at 280 K, (c) after 2 h at 298 K, (d) after workup at 298 K (see Supporting Information for a larger temperature range spectra) (i, unidentified impurities).

NMR spectrum of **2** exhibits an AB splitting pattern, indicating two nonequivalent P atoms. The deprotonated "arm" of **2** gives rise to a signal at 4.15 ppm in the ^{1}H NMR spectrum, corresponding to one proton, and a CH doublet signal at 73.46 ppm ($^1J_{PC}$ = 55.4 Hz) in the ^{13}CQDEPT spectrum. The hydrides give rise to a single triplet signal at −26.35 ($^2J_{PH}$ = 10.1 Hz), integrating to 2H, similar to the hydrides of complex **1**.[33]

Complex **3** exhibits a symmetric ^{1}H and ^{13}C NMR spectral pattern of the ligand backbone, and a singlet signal in the ^{31}P{^{1}H} NMR spectrum at 76.81 ppm, as expected for an aromatic square planar complex. The hydride of complex **3** gives rise to a triplet signal at −11.10 ($^2J_{PH}$ = 17.3 Hz), integrating to 1H. The X-ray structure of **3** (Figure 2), in which the hydride was located, reveals a distorted square planar geometry with Ir−H(1) bond length of 1.48(5) Å. Complex **3** is a rare example of a square planar Ir(I) monohydride. To the best of our knowledge, only two other isolated four-coordinated Ir(I) monohydride complexes were previously reported, a pincer pyridine−dicarbene−Iridium mono hydride complex ((CNHC−N−CNHC)IrH) was reported by Danopoulos et al.[34] and the complex [IrH(N$_2$)(PmAd(^{i}Pr)$_2$)$_2$] (mAd = methylene-1-adamantyl) was reported by Figueroa et al.[35] While complex **2** was found to be unstable at ambient temperature, Nozaki et al. reported that the ^{i}Pr analogue of **2** is stable and does not aromatize to the monohydride complex.[21a]

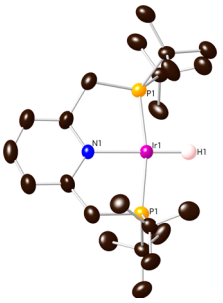

Figure 2. Crystal structure of complex **3** at 50% probability level. Hydrogen atoms (with the exception of H1) are omitted for clarity. Symmetry transformations used to generate equivalent atoms. Selected bond lengths (Å) and angles (deg): N(1)−Ir(1), 2.049(8); P(1)−Ir(1), 2.2406(13); H(1)−Ir(1), 1.48(5); N(1)−Ir(1)−P(1), 84.38(11); N(1)−Ir(1)−H(1), 180.000(18); H(1)−Ir(1)−P(1), 95.62(11).

DFT calculations (SMD(THF)-DSD-PBEB86-D3BJ/def2-TZVP//BP86-D3/def2-SV(P)) conducted on the actual complexes **2** and **3** show that **3** is more stable than **2** (by 3.9 kcal/mol).[36] Although complex **3** is the thermodynamic product of deprotonation of **1**, it could not be formed exclusively, and was always obtained as a major component in a mixture with complex **2** in a ratio of about 7:3.[37] Spin saturation transfer (SST) experiments were conducted on a crude sample of **2** and **3**, which was obtained *in situ* by addition of KHMDS to complex **1**, as well as on a "worked-up" sample, free of the conjugated acid and salt (Figure 3). The SST of the crude sample showed a clear proton exchange between the

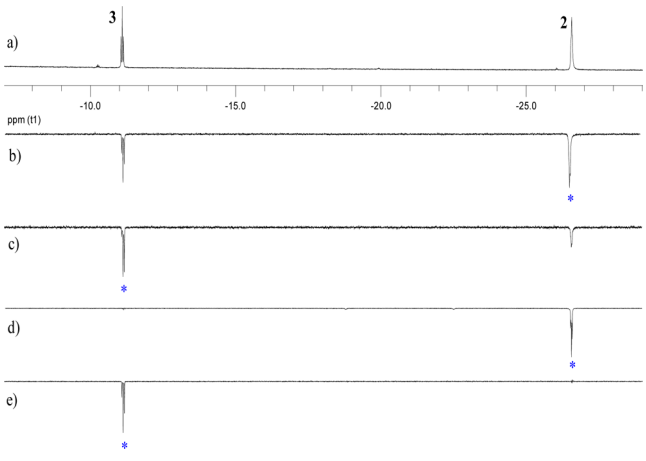

Figure 3. Spin saturation transfer (SST) experiments with complexes **2** and **3**. (a) ^{1}H NMR spectrum of **2** and **3** (hydride region) in toluene-d_8. (b and c) Spin saturation of the hydrides of complexes **2** and **3**, respectively, of a crude sample. (d and e) Spin saturation of hydrides of complexes **2** and **3**, respectively, of a "worked-up" sample. Saturated signals denoted by an asterisk (*) (see Supporting Information for SST experiments which include the PNP ligand protons).

DOI: 10.1021/jacs.6b00202
J. Am. Chem. Soc. 2016, 138, 6445−6454

hydrides, as well as between the hydrides and the benzylic positions of **2** and **3**. However, when an SST experiment was conducted on a "worked-up" sample of **2** and **3** (in the absence of the formed conjugate acid HMDS), no proton exchange between **2** and **3** was observed. Thus, we concluded that the exchange between **2** and **3** required a proton transfer assistant, such as HMDS or water.

CO_2 Reductive Cleavage by Complexes 2 and 3. A mixture of complexes **2** and **3** reacts with CO at ambient temperature to release H_2 by MLC, resulting in the dearomatized carbonyl complex [(^{t}Bu-PNP*)Ir(CO)] (**4**)[32] exclusively (Scheme 2). Similar MLC reactivity with CO was

Scheme 2. Reactivity of 2 and 3 with CO and CO_2

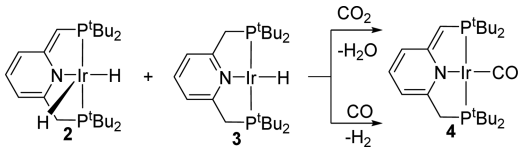

observed in [(^{t}Bu-PNP)CoH].[19c] Surprisingly, reaction of complexes **2** and **3** with CO_2 (1 equiv[38] or excess up to ca. 1500 equiv (2 bar)) resulted in the formation of **4**, while the related complexes [(^{t}Bu-PNP)CoH],[19c] [(POCOP)Ir(H)$_2$][20b] (POCOP = C_6H_4-1,3-[OP^{t}Bu$_2$]), [(PCP)Ir(H)$_2$][20b] (PCP = C_6H_4-1,3-[CH_2P^{t}Bu$_2$]), [(HN(^{i}Pr$_2$PC_2H_4)$_2$)Ir(H)$_3$],[20a] and [(^{i}Pr-PNP)Ir(H)$_3$][21] were reported to yield a formato complex upon reaction with CO_2. A DFT study by Hazari and co-workers[20a] suggests that more nucleophilic hydrides undergo CO_2 insertion more readily. The hydrides in complexes **2** and **3** are possibly weaker nucleophiles; hence, CO_2 insertion to yield a formato complex was not observed.

To shed light on the reaction mechanism of CO_2 reduction to CO by complexes **2** and **3**, the reaction progress was followed at ambient and low temperatures. Upon addition of CO_2 to complexes **2** and **3** at 195 K, a new complex was identified (**5**) (Scheme 3). Complex **5** is obtained by a

Scheme 3. Reaction Pathway of Complexes 2 and 3 with CO_2 To Give Complexes 4, 5, and 6

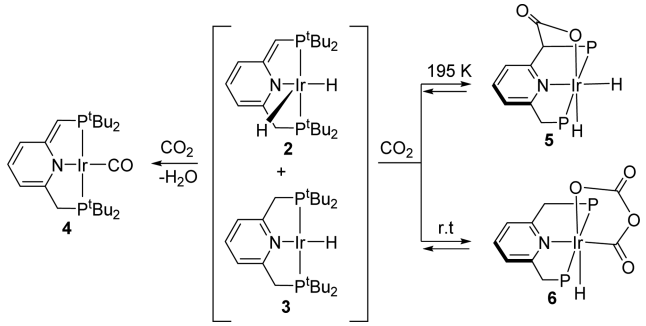

concerted [1,3]-addition of CO_2 to the exocyclic carbon of a dearomatized pincer ligand, resulting in the formation of new C–C and Ir–O bonds. This mode of CO_2 activation by MLC was previously reported to take place reversibly by ^{t}Bu-PNP Ru and Re complexes as well as by a PNN Ru complex (PNN = 2-(CH_2–P^{t}Bu$_2$)-6-(CH_2–NEt_2)C_5H_3N).[26−28] While complex **5** could be obtained at low temperature (195 K), after 3 h at ambient temperature, only complex **4** was detected (Figure 4). The ^{31}P{^{1}H} NMR spectrum of **5** exhibits an AB splitting

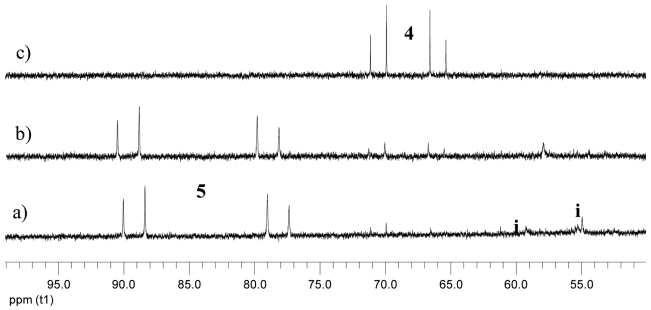

Figure 4. Variable temperature ^{31}P{^{1}H} NMR spectra (202 MHz) of the reaction mixture of **2** and **3** with CO_2 in toluene-d_8 to give **4** and **5**: (a) 220 K, (b) after 30 min at 283 K, (c) after 3 h at 298 K (i, unidentified intermediates).

pattern, indicating two nonequivalent P atoms. The ^{1}H NMR of **5** exhibits two hydride signals which appear as a doublet of triplets at −26.08 ($^2J_{HP}$ = 17.9 Hz, $^2J_{HH}$ = 8.6 Hz) and −17.82 ($^2J_{HP}$ = 12.9 Hz, $^2J_{HH}$ = 8.6 Hz). The CO_2 carbon gives rise to a singlet signal at 170.9 ppm. Labeled complex **5**-^{13}**C**O_2 exhibits in the HMBC 2D NMR a correlation between the benzylic proton (P-CH-Py) and the CO_2 carbon, confirming the C–C bond between the CO_2 and the benzylic position.

1,3-Addition of CO_2 to ^{t}Bu-PNP Ru,[26] Re,[27] and to the phosphine arm of PNN Ru[28] complexes was found to be reversible at ambient or elevated temperatures. Complex **5**-^{12}**C**O_2 (prepared *in situ*) did not exhibit exchange with additional $^{13}CO_2$ at 273 K; however, at ambient temperature, complex **4**-^{13}**CO** was obtained, according to ^{13}CQDEPT. Thus, complex **5** is reversibly formed.

Complexes **2** and **3** reacted instantly with CO_2 at ambient temperature in benzene, toluene, or THF to give a brown solution and a white precipitate. Gradually, after standing overnight, the reaction mixture turned red and most of the precipitate disappeared. Upon vacuum application on the reaction mixture, a red solid was formed and was dissolved in benzene to give a clear red solution of complex **4**.[39] Following the reaction progress with 1 and 10 equiv of CO_2 in benzene by ^{31}P{^{1}H} NMR showed that in both reactions complex **4** was formed spontaneously. Signals of complex **5** were also detected immediately after CO_2 addition; however, they disappeared after 2 h.[40] The reaction progress was 1.5 times faster with only 1 equiv of CO_2, while more precipitation was observed (qualitatively) with 10 equiv of CO_2. In both reactions, complex **4** was obtained quantitatively after vacuum was applied on the reaction mixture. If vacuum was not applied, complex **4** was obtained in 90% and 80% yield in the reactions with 1 and 10 equiv of CO_2, respectively, whereas the remaining was an insoluble white precipitate. The white precipitate was isolated and identified by NMR and X-ray analysis as [(^{t}Bu-PNP)Ir-(H)(C_2O_4-$\kappa_{C,O}$)] (**6**, Scheme 3). Complex **6** is a rare example of a metallacycle formed by reductive coupling of two CO_2 molecules. Only two characterized C_2O_4-$\kappa_{C,O}$ Ir complexes were reported,[8] although it was suggested also for a Rh complex.[9] While complex **6** was formed as a minor product (10% yield in the reaction with 1 equiv of CO_2), when a large excess of CO_2 was added (18 equiv), complex **6** could be obtained in 35% yield by precipitation with pentane. Complex **6** is soluble in acetone and methylene chloride; however, it is not stable in these solvents at ambient temperature, and decomposes to give a mixture of unidentified complexes. Similar behavior was reported by Oro and Langer et al.[8a]

DOI: 10.1021/jacs.6b00202
J. Am. Chem. Soc. 2016, 138, 6445−6454

Complex **6** is reversibly formed, and CO_2 removal from complex **6** by vacuum resulted in the formation of complex **4**.

Crystals suitable for X-ray analysis of **6** were obtained by layering pentane over an acetone or methylene chloride concentrated solution of **6** at −35 °C. The X-ray structure of complex **6** (Figure 5) reveals an octahedral geometry, with the

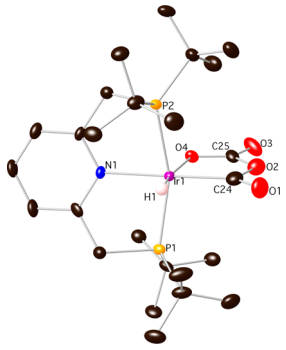

Figure 5. Crystal structure of complex **6** at 50% probability level. Hydrogen atoms (with the exception of H1) are omitted for clarity. Selected bond lengths (Å) and angles (deg): N(1)−Ir(1), 2.140(2); P(1)−Ir(1), 2.3245(7); H(1)−Ir(1), 1.43(3); O(4)−Ir(1), 2.1762(19); C(24)−Ir(1), 1.976(3); O(1)−C(24), 1.209(4); O(2)−C(24), 1.445(3); O(2)−C(25), 1.392(4); O(3)−C(25), 1.227(4); O(4)−C(25), 1.270(3); N(1)−Ir(1)−C(24), 177.06(10); P(1)−Ir(1)−P(2), 159.92(3); O(4)−Ir(1)−H(1), 175.3(13).

hydride ligand located *trans* to an oxygen atom of the C_2O_4-$\kappa_{C,O}$ ligand. The bond lengths of the metallacycle moiety in complex **6** are similar to the bond lengths of the two reported X-ray structures [*mer*-IrCl(PR_3)(C_2O_4-$\kappa_{C,O}$)] (R = PMe_3, $PPhMe_2$), with the exception of the Ir−O(4) bond length, which is elongated by 0.06 Å. This elongation can be explained by the strong trans influence of the hydride ligand, which is located *trans* to O(4), while in the reported structures, the relevant O atom is *trans* to a phosphine ligand.

NMR characterization of **6** was possible by low-temperature measurements in methylene chloride or acetone. Complex **6** gives rise to a singlet signal at 52.11 ppm in the $^{31}P\{^1H\}$ NMR spectrum, indicative of an aromatized complex. The hydride ligand exhibits a triplet at −22.20 ppm in the ^1H NMR with $^2J_{PH}$ = 13.9 Hz, and a doublet of triplets with an additional coupling of $^2J_{CH}$ = 3.8 Hz when $^{13}CO_2$ was applied. The C_2O_4-$\kappa_{C,O}$ ligand gives rise to a broad triplet signal at 169.2 ppm (Ir−C, $^2J_{PC}$ = 7 Hz) and a singlet signal at 161.17 ppm (Ir−O−C), and infrared bands at 1705.8, 1664.6, and 1284.5 cm^{-1}. With the use of $^{13}CO_2$, a red shift was observed with bands at 1662.6, 1610.1, and 1260.7 cm^{-1}. The reported chemical shifts and IR bands for the related complex [*mer*-IrCl($PPhMe_2$)(C_2O_4-$\kappa_{C,O}$)] are slightly different, with signals at 159.3 and 158.8 ppm in the $^{13}C\{^1H\}$ NMR and IR bands at 1727, 1686, 1278, and 999 cm^{-1}. For the related complex [*mer*-IrCl(PMe_3)(C_2O_4-$\kappa_{C,O}$)] IR bands at 1725, 1680, 1648, 1605, 1290, 1005 were reported. The differences in the spectroscopic values of the complexes [*mer*-IrCl(PR_3)(C_2O_4-$\kappa_{C,O}$)] (R = PMe_3, $PPhMe_2$) and complex **6** may result from the different arrangement of the ligands located *trans* to the ligand C_2O_4-$\kappa_{C,O}$, as was observed also in the X-ray structure.

The reactive intermediate in the formation of C_2O_4-$\kappa_{C,O}$ metallacycle was suggested by Herskovitz et al.[8b] experimentally and by Oro and Langer et al.[8a] computationally to be an η^1−CO_2 complex. Although we could not identify an η^1−CO_2 intermediate in the reaction mixture, it is likely that such an intermediate leads to formation of both complexes **4** and **6**. However, on the basis of the X-ray structure of complex **6**, in which the hydride is *trans* to an oxygen atom of the C_2O_4-$\kappa_{C,O}$ ligand, the intermediate leading to complex **6** should be an η^1−CO_2 complex in which the CO_2 is *trans* to the pyridine group and the hydride is at the apical position (intermediate ***7trans***, Scheme 4). Since coordination of CO_2 to complexes **2** and **3**

Scheme 4. Proposed η^1−CO_2 Intermediates in the Formation of Complexes 4 and 6

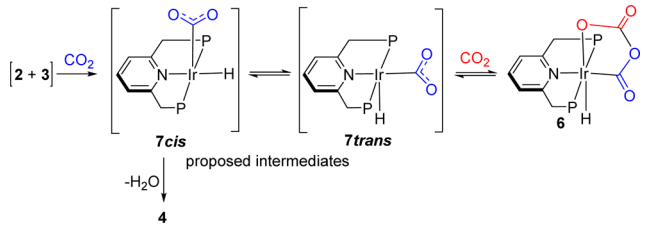

would give the η^1−CO_2 *cis*-intermediate (***7cis***, Scheme 4), in which CO_2 is at the apical position, isomerization from ***7cis*** to ***7trans*** has to take place prior to formation of **6**. DFT calculations predict that ***7trans*** is less stable by 1.3 kcal/mol than ***7cis***, with a conversion barrier of 8.6 kcal/mol. The calculated η^2−CO_2 isomer was less stable by about 20 kcal/mol than **7**.

A plausible mechanism for the formation of **4** involves intermediate ***7cis***, in which the nucleophilic oxygen of the CO_2 ligand at the apical position is in proximity to the benzylic position. Intramolecular deprotonation of the PNP ligand by the coordinated CO_2 molecule leads to an unstable metalo carboxylate hydrido intermediate (**8**, Figure 6). Decomposition of the latter yields complex **4** and water. Following the reaction of **2** and **3** with CO_2 in THF-d_8, we observed the buildup of a broad water signal (see Supporting Information). It is important to note that under all reaction conditions (low and ambient temperatures, polar and apolar solvents, 1 equiv or excess of CO_2), a formato intermediate was not detected.

The reaction of complexes **2** and **3** can take place quantitatively with only 1 equiv of CO_2.[38] Thus, we excluded a bimolecular O-transfer mechanism, in which an oxygen atom is transferred from the metal−η^1−CO_2 intermediate to an oxygen acceptor such as free CO_2, hydride, phosphine ligands or to the metal.[23,24]

Reaction of complexes **2** and **3** with CO_2 in acetone rather than benzene, toluene, or THF also resulted in the formation of complex **4**. However, following the reaction at low temperatures, complex **5** was not detected, while complex **6** was observed along with two other unidentified intermediates. It is likely that the benzylic dearomatized position is protonated in acetone,[32] retarding the 1,3 concerted addition of CO_2. The observation that complex **4** was obtained also in the absence of **5** suggests that complex **5** is a reversibly formed resting state. A similar effect was reported by Pidko and co-workers, in which the 1,3-addition of CO_2 to [(^{t}Bu-PNP*)Ru(H)(CO)] was observed to inhibit the catalytic CO_2 hydrogenation to formic acid.[20i]

DFT Calculations. DFT calculations were performed in order to gain more insight into the mechanism of CO_2 cleavage by complexes **2** and **3**. The free energy surface in a simulated THF solvent is shown in Figure 6 along with a schematic

DOI: 10.1021/jacs.6b00202
J. Am. Chem. Soc. 2016, 138, 6445−6454

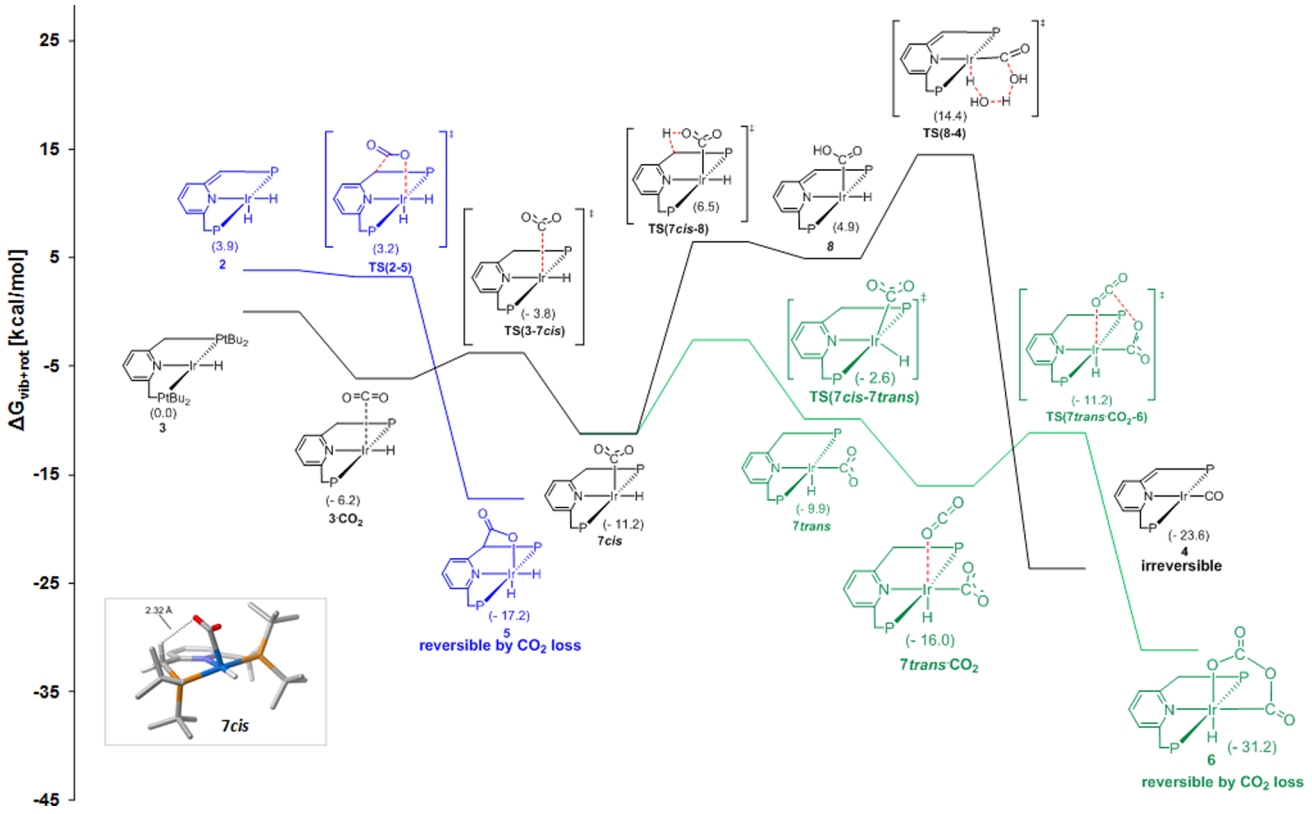

Figure 6. Reaction profile of complexes **2** and **3** with CO_2 to give complexes **4**, **5**, and **6**. (SMD(THF)-DSD-PBEB86-D3BJ/def2-TZVP//BP86-D3/def2-SV(P)). Annotation: P = P^{t}Bu$_2$. Inset: Calculated structure of ***7cis*** with CH−O hydrogen bond shown.

illustration of intermediates and transition states that were located. Three possible reaction pathways are described, starting from complex **2** to give complex **5** (described in blue) or from complex **3** to give complex **4** (described in black) or **6** (described in green). Thus, the DFT calculations are in agreement with the experimental findings, which indicate that complexes **5** and **6** are reversibly formed and are not intermediates in the formation of complex **4**.

Starting from complex **3**, coordination of CO_2 to the Ir center leads to a relatively stable intermediate ***7cis***. Hydrogen bonding between the acidic benzylic proton and the O atom of the bound CO_2 in complex ***7cis*** leads to the formation of an Ir carboxylate intermediate **8**. The latter eliminates water to give the carbonyl complex **4**. Introducing a water molecule to the last transition state [**TS(8−4)**] assists the hydrogen transfer process and lowers the transition state by 10 kcal/mol. H-transfer facilitated by water was predicted in similar transformations by DFT.[21b,32,41]

The calculated HOMO orbital of complex **3** exhibits a d_{z^2} orbital on the Ir(I) center (Figure 7), in line with a nucleophilic attack of Ir(I) on CO_2 to give intermediate ***7cis***. The HOMO representation of complex **2** exhibits the highest coefficient at the deprotonated benzylic position, in line with the observed 1,3-addition of CO_2 to give complex **5**.

A possible pathway for the formation of complex **6** was also calculated (Figure 6, in green). The optimized structure of **6** fits well with its X-ray structure (see Supporting Information). Starting from intermediate ***7cis***, which is the active intermediate in the formation of **4**, isomerization to the intermediate ***7trans*** takes place. Coordination of a second CO_2 molecule allows coupling of the two CO_2 ligands, as depicted in the located transition state **TS(7trans·CO$_2$-6)**. The formation of ***7trans*** from **6** via **TS(7trans·CO$_2$-6)** requires an activation barrier of only 20 kcal/mol, while the reverse reaction of **4** via **TS(8−4)** has an activation barrier of 38 kcal/mol. Thus, although complex **6** was found to be more stable than complex **4** by 7.6 kcal/mol, complex **6** can be reversibly formed at room temperature by removing CO_2 from the reaction mixture, while complex **4** is formed irreversibly.[42]

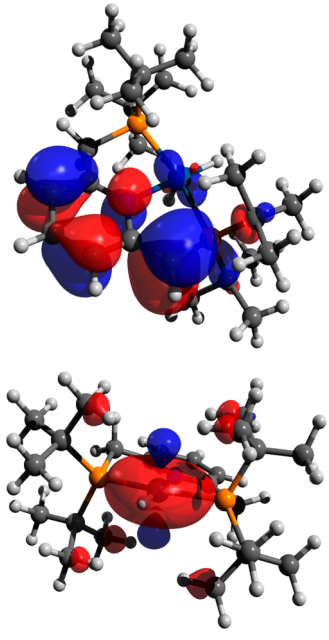

Figure 7. Highest occupied Kohn−Sham molecular orbital (HOMO) of complex **2** (top) and **3** (bottom).

DOI: 10.1021/jacs.6b00202
J. Am. Chem. Soc. 2016, 138, 6445−6454

CONCLUSIONS

In summary, we have presented a new mode of CO_2 reductive cleavage to CO and water involving metal−ligand-cooperation. Deprotonation of the reported complex [(^{t}Bu-PNP)Ir(H)$_2$]-[PF_6] (**1**)[33] results in the kinetic dearomatized product [(^{t}Bu-PNP*)Ir(H)$_2$] (**2**) and in the thermodynamic aromatized product [(^{t}Bu-PNP)Ir(H)] (**3**). Complex **3** is a rare example of a square planar Ir(I) monohydride complex. A mixture of **2** and **3** reacts with CO to give exclusively the dearomatized complex [(^{t}Bu-PNP*)Ir(CO)] (**4**) and dihydrogen by metal−ligand-cooperation. Unexpectedly, complex **4** was also obtained by reaction of **2** and **3** with CO_2. Following the reaction progress with CO_2, a reversible 1,3-addition of CO_2 to the benzylic position was observed, yielding complex [(^{t}Bu-PNP-COO)Ir-(H)$_2$] (**5**) as a kinetic product. A rare di-CO_2 metallacycle complex [(^{t}Bu-PNP)Ir(H)(C_2O_4-$\kappa_{C,O}$)] (**6**) was also observed to form reversibly, while the final products in the reaction of complexes **2** and **3** with CO_2 are water and complex **4**. DFT calculations predict that **5** and **6** are formed reversibly, and are not intermediates in the formation of **4**, which is the thermodynamic product. The calculations support a metal−ligand-cooperation pathway in which intramolecular deprotonation of the benzylic position by the CO_2 adduct in an η^1−CO_2 intermediate leads to a carboxylate intermediate, which further reacts with the hydride ligand to give complex **4** and water. The reactivity of complexes **2** and **3** in activation of oxygen, water, and amines is currently being explored. We are also studying the possibility of utilization of CO_2 reductive cleavage via MLC catalytically.

EXPERIMENTAL SECTION

General Procedures. All experiments with metal complexes and phosphine ligands were carried out under a purified nitrogen atmosphere in a Vacuum Atmosphere glovebox equipped with an MO 40-2 inert gas purifier or using standard Schlenk techniques. All solvents were reagent grade or better. All nondeuterated solvents were refluxed over sodium/benzophenone ketyl and distilled under an argon atmosphere. Methylene chloride and acetone were used as received and dried over 4 Å molecular sieves and calcium sulfate, respectively. [(^{t}Bu-PNP)Ir(H)$_2$][PF_6] (**1**) was prepared according to literature procedures.[33] Deuterated solvents were used as received. All the solvents were degassed with argon and kept in the glovebox over 4 Å molecular sieves (acetone was kept over calcium sulfate). Commercially available reagents were used as received. ^{1}H, ^{13}C, and ^{31}P NMR spectra were recorded using a Bruker Avance III-300, Bruker Avance III-400 or Avance 500 NMR spectrometer. All spectra were recorded at 298 K unless otherwise indicated. ^{1}H NMR and ^{13}C{^{1}H} NMR chemical shifts are reported in parts per million (ppm) downfield from tetramethylsilane. In ^{1}H NMR, the chemical shifts were referenced to the residual hydrogen signal of the deuterated solvents. In ^{13}C{^{1}H} NMR measurements, the signals of deuterated solvents were used as a reference. ^{31}P NMR chemical shifts are reported in parts per million downfield from H_3PO_4 and referenced to an external 85% solution of phosphoric acid in D_2O. Abbreviations used in the description of NMR data are as follows: br, broad; s, singlet; d, doublet; t, triplet; q, quartet; m, multiplet; v, virtual. Temperature calibration of the spectrometer was performed using CH_3OH/CD_3OD. IR spectra were recorded on Thermo Nicolet 6700 FT-IR.

Synthesis of [(^{t}Bu-PNP*)Ir(H)$_2$] (2). A suspension of complex **1** (9.6 mg, 0.013 mmol) in toluene-d_8 (0.2 mL) was placed in an NMR tube equipped with a septum. The NMR tube was cooled to 195 K (dry ice/acetone bath) and a cold (195 K) solution of KHMDS (2.6 mg, 0.013 mmol) in toluene-d_8 (0.3 mL) was injected to the sample. The resulting cold mixture was shaken for a few seconds to give a red brownish solution (some of the starting complex remained as a solid in the NMR tube due to low solubility in toluene). The sample was placed in an NMR spectrometer which was precooled to 230 K, showing exclusive formation of complex **2** at this temperature.

^{31}P{^{1}H} NMR (202 MHz, toluene-d_8, 230 K) δ: AB system centered at 73.08 (d, $^2J_{PP}$ = 291.6 Hz) and 66.34 (d, $^2J_{PP}$ = 291.6 Hz). ^{1}H NMR (500 MHz, toluene-d_8, 220 K) δ: −26.35 (t, 2H, $^2J_{PH}$ = 10.1 Hz, Ir−H), 1.02 (d, 18H, $^3J_{PH}$ = 12.9 Hz, P−C(CH_3)$_3$), 1.45 (d, 18H, $^3J_{PH}$ = 12.9 Hz, P−C(CH_3)$_3$), 2.75 (d, 2H, $^2J_{PH}$ = 8.6 Hz, P-CH_2Py), 4.15 (br vt, 1H, J_{PH} = 2.6 Hz, P-*CH*Py), 5.46 (d, 1H, $^3J_{HH}$ = 6.3 Hz, Py-H), 6.43 (m, 1H, Py-H), 6.52 (m, 1H, Py-H). ^{13}C{^{1}H} NMR (101 MHz, toluene-d_8, 220 K) δ: 28.83 (br s, P−C(CH_3)$_3$), 29.49 (br s, P−C(CH_3)$_3$), 34.21 (br d, $^1J_{PC}$ = 19.7 Hz, P-*C*(CH_3)$_3$), 35.82 (dd, $^1J_{PC}$ = 26.8 Hz, $^3J_{PC}$ = 2.7 Hz, P-*C*(CH_3)$_3$), 36.78 (d, $^1J_{PC}$ = 20.7 Hz, CH_2P), 73.46 (d, $^1J_{PC}$ = 55.4 Hz, CHP), 96.33 (d, $^3J_{PC}$ = 10.3 Hz, Py-CH), 115.36 (d, $^3J_{PC}$ = 17.2 Hz, Py-CH), 132.23 (s, Py-CH), 163.86 (br s, Py-C), 174.53 (br m, Py-C). Complex **2** is unstable at ambient temperatures and was not isolated. The NMR spectra of **2** appear in the Supporting Information. IR (for a mixture of **2** and **3**) (ν_{Ir-H}): 2359, 2340 cm^{-1}.

Synthesis of [(^{t}Bu-PNP)IrH] (3). A ^{t}BuOK (16.0 mg, 0.143 mmol) solution (THF, 5 mL) was added to a suspension of complex **1** (104.9 mg, 0.143 mmol) in THF (3 mL). The reaction mixture was stirred vigorously until all the yellow suspension (complex **1**) disappeared (about 30 min), and a dark purple solution was obtained. The solvent was removed under vacuum. The residue was extracted with benzene, and the extracts were combined and filtered through a 0.2 μm Teflon filter. The solvent was removed under vacuum to give a mixture of complexes **2** and **3** as a black solid (68.3 mg) in 80% yield. Acceptable elemental analysis for **3** could not be obtained. The assignment of the signals of complex **3** was done based on the mixture (see Supporting Information). Complexes **2** and **3** are unstable in solution at ambient temperature, and the mixture was stored as a solid at −30 °C under inert atmosphere (in the glovebox). For the impurities which appear in solution after workup, see Supporting Information. Crystals suitable for X-ray analysis were obtained from a concentrated solution of **2** and **3** in toluene at −30 °C.

^{31}P{^{1}H} NMR (121 MHz, toluene-d_8, 298 K) δ: 76.81 (s). ^{1}H NMR (500 MHz, toluene-d_8, 298 K) δ: −11.10 (t, 1H, $^2J_{PH}$ = 17.3 Hz, Ir−H), 1.37 (vt, 36H, J_{PH} = 6.2 Hz, P−C(CH_3)$_3$), 2.32 (br s, 4H, P-CH_2Py), 6.40 (d, 2H, $^3J_{HH}$ = 7.5 Hz, Py-H), 7.98 (t, 1H, $^3J_{HH}$ = 7.5 Hz, Py-H). ^{13}C{^{1}H} NMR (126 MHz, toluene-d_8, 298 K): 29.61 (vt, J_{PC} = 3.7 Hz, P−C(CH_3)$_3$), 34.52 (vt, J_{PC} = 9.8 Hz, P-*C*(CH_3)$_3$), 39.61 (vt, J_{PC} = 7.2 Hz, CH_2P), 120.84 (vt, J_{PC} = 4.9 Hz, Py-CH), 125.42 (s, Py-CH), 162.30 (vt, J_{PC} = 6.1 Hz, Py-C).

X-ray Structural Analysis of **3**. Crystal Data: $C_{23}H_{44}IrNP_2$, dark red chunk, 0.31 × 0.19 × 0.19 mm^3, tetragonal, $P4_2nm$, $a = b = 11.527(2)$ Å, $c = 9.5824(19)$ Å, from 7619 reflections, $T = 100(2)$ K, $V = 1273.2(5)$ Å^3, $Z = 2$, Fw = 588.73, Dc = 1.536 Mg/m^{-3}, $\mu = 5.377$ mm^{-1}.

Data Collection and Processing. Bruker APEX-II Kappa CCD diffractometer, Mo Kα (λ = 0.71073 Å), graphite monochromator, $-16 \le h \le 16$, $-16 \le k \le 16$, $-13 \le l \le 0$, frame scan width = 0.5°, scan speed 1.0° per 60 s, typical peak mosaicity 0.66°, 7619 reflections collected, 1092 independent reflections (R_{int} = 0.0245). The data were processed with SAINT.

Solution and Refinement. Structure solved with AUTOSTRUCTURE module. Full matrix least-squares refinement based on F^2 with SHELXL-97 on 120 parameters with 2 restraints gave final R1 = 0.0231 (based on F^2) for data with $I > 2\sigma(I)$, R1 = 0.0279 on 1092 reflections, goodness-of-fit on F^2 = 1.258, largest electron density peak = 1.071 e Å^{-3}, and largest hole = −0.290 e Å^{-3}.

Spin Saturation Transfer (SST) Experiments. Spin saturation transfer experiments were performed on a mixture of complexes **2** and **3** in benzene-d_6. Each experiment involved selective spin saturation at the hydride. The response was detected by comparison (difference spectrum) with a control experiment in which the sample was irradiated off-resonance under the same conditions.

Reaction of complexes 2 and 3 with CO. A benzene-d_6 solution (0.5 mL) of complexes **2** and **3** (8.5 mg, 0.014 mmol) was placed in a J. Young NMR tube and the nitrogen atmosphere was replaced by CO.

DOI: 10.1021/jacs.6b00202
J. Am. Chem. Soc. 2016, 138, 6445−6454

A red clear solution of complex **4**[32] was obtained immediately in quantitative yield according to $^{31}P\{^{1}H\}$ NMR.

Reaction of complexes 2 and 3 with CO_2. *1. Reaction with 1 and 10 equiv of CO_2 at Ambient Temperature in Benzene.* Two NMR tubes equipped with septa were charged with benzene-d_6 solutions (0.5 mL) containing a mixture of complexes **2** and **3** in a 3:7 ratio, respectively (0.024 M, 0.012 mmol). 1 or 10 equiv of CO_2 were injected to the NMR tubes (269 μL, ~1 equiv; 2.7 mL, ~10 equiv) and the NMR tubes were shaken vigorously for a few seconds. The solutions' color turned immediately to light brown and then to red, and a white precipitate was formed in both tubes. The reaction progress was monitored by $^{31}P\{^{1}H\}$ NMR. After 18 h, the samples were dried under vacuum and the resulting solid in both samples was redissolved in benzene-d_6 or methylene chloride-d_2 to give a clear red solutions of complex **4**, in quantitative yield, according to $^{31}P\{^{1}H\}$ NMR. When the reactions were conducted with filtration of the white precipitate after 18 h (instead of applying vacuum on the crude reaction), complex **4** was obtained in 90% and 80% yield for 1 and 10 equiv of CO_2, respectively. For the $^{31}P\{^{1}H\}$ NMR spectra of the reaction progress, see Supporting Information.

2. Reaction in THF and Detection of Water. A THF-d_8 solution (0.5 mL) of complexes **2** and **3** (18 mg, 0.03 mmol) was placed in an NMR tube equipped with a septum. CO_2 was added via syringe (2.5 mL, ~0.11 mmol), and the NMR tube was shaken vigorously for a few seconds. The solution color turned immediately to light brown and then to red, and a white precipitate was formed. The reaction progress was monitored by ^{1}H and $^{31}P\{^{1}H\}$ NMR. A broad signal of water at 2.5 ppm was observed after 5 h of CO_2 addition, concomitant with the formation of complex **4**. After 18 h, the reaction mixture was dried under vacuum and the resulting red solid was redissolved in THF-d_8 to give a clear red solution. The ^{1}H NMR spectrum of the reaction mixture after vacuum was missing only the signal at 2.5 ppm which was assigned as water.[43] For the NMR spectra, see Supporting Information.

3. Reaction in Acetone. An acetone-d_6 solution (0.5 mL) of complexes **2** and **3** (7 mg, 0.012 mmol) was placed in an NMR tube equipped with a septum and was cooled to 195 K using a dry ice/acetone bath. $^{13}CO_2$ (1 mL, ~0.045 mmol) was injected into the NMR tube, and the resulting cold mixture was shaken for a few seconds. The color turned from deep purple to brown. The sample was quickly returned to the dry ice/acetone bath and then transferred into an NMR spectrometer precooled to 220 K. The reaction mixture was gradually heated to 298 K in the NMR spectrometer, and the reaction progress was followed by $^{31}P\{^{1}H\}$, ^{1}H and $^{13}C\{^{1}H\}$ NMR. Complex **4** was obtained in 80% yield according to $^{31}P\{^{1}H\}$ NMR along with unidentified impurities and 1% of the cationic complex, $[(^{t}Bu\text{-}PNP)IrCO]^{+}$.[33]

Characterization of [(^{t}Bu-PNP-COO)Ir(H)$_2$] (5). A toluene-d_8 solution (0.5 mL) of complexes **2** and **3** (7 mg, 0.012 mmol) was placed in an NMR tube equipped with a septum and, the tube was cooled to 195 K using a dry ice/acetone bath. $^{13}CO_2$ (0.5 mL, 0.022 mmol) was injected into the NMR tube, and the resulting cold mixture was shaken for a few seconds. The color turned from deep purple to brown, and a precipitate was formed (assumed as complex **6**). The sample was quickly returned to the dry ice/acetone bath and then transferred into an NMR spectrometer precooled to 220 K. NMR data of the sample was recorded at variable temperatures in the range of 220–298 K. Complex **5** is not stable at ambient temperature and already at 283 K signals of complex **4** were observed (Figure 4). According to $^{31}P\{^{1}H\}$ NMR, the signals of complex **5** disappeared after 3 h at ambient temperature. The NMR spectra of **5** appear in the Supporting Information. Partial characterization was possible *in situ*, with the aid of 2D NMR techniques.

$^{31}P\{^{1}H\}$ NMR (202 MHz, toluene-d_8, 220 K) δ: AB system centered at 89.3 (br d, $^{2}J_{PP}$ = 335 Hz) and 78.5 (d, $^{2}J_{PP}$ = 335 Hz). ^{1}H NMR (500 MHz, toluene-d_8, 250 K) δ: −26.11 (m, 1H, at 298 K the signal appears at −26.08 (td, $^{2}J_{HP}$ = 17.9 Hz, $^{2}J_{HH}$ = 8.6 Hz), Ir−H), −17.8 (br m, 1H, at 298 K the signal appears at −17.82 (dt, 1H, $^{2}J_{HP}$ = 12.9 Hz, $^{2}J_{HH}$ = 8.6 Hz), Ir−H), 0.87 (d, 9H, $^{3}J_{PH}$ = 12.3 Hz, P−C(CH_3)$_3$), 0.97 (d, 9H, $^{3}J_{PH}$ = 13.0 Hz, P−C(CH_3)$_3$), 1.21 (d, 9H, $^{3}J_{PH}$ = 13.0 Hz, P−C(CH_3)$_3$), 1.60 (d, 9H, $^{3}J_{PH}$ = 13.0 Hz, P−C(CH_3)$_3$), 2.53 (dd, 1H, $^{2}J_{PH}$ = 6.3 Hz, $^{2}J_{HH}$ = 15.5 Hz, P-CH_2Py), 3.13 (br dd, 1H, $^{2}J_{PH}$ = 10 Hz, $^{2}J_{HH}$ = 15 Hz, P-CH_2Py), 5.09 (br s, 1H, P-CH-Py), 6.36 (m, 1H, Py-H), 6.50 (d, 1H, $^{3}J_{HH}$ = 7.2 Hz, Py-H), 6.86 (m, 1H, $^{3}J_{HH}$ = 6.6 Hz, Py-H). $^{13}C\{^{1}H\}$ NMR (101 MHz, toluene-d_8, 220 K) δ: 28.88 (d, $^{2}J_{PC}$ = 4.1 Hz, P−C(CH_3)$_3$), 29.42 (d, $^{2}J_{PC}$ = 4.1 Hz, P−C(CH_3)$_3$), 29.70 (d, $^{2}J_{PC}$ = 4.6 Hz, P−C(CH_3)$_3$), 30.31 (d, $^{2}J_{PC}$ = 4.4 Hz, P−C(CH_3)$_3$), 38.5 (m, CH_2P), 64.1 (br s, CHP), 170.85 (d, $^{2}J_{PC}$ = 7.2 Hz, CO). The following signals could not be assigned due to the low concentration of complex **5** in solution: all Pyridine and P-C(CH_3)$_3$) carbons.

Characterization of [(^{t}Bu-PNP)Ir(C_2O_4-$\kappa_{C,O}$)H] (6). A benzene or THF solution (2 mL) of complexes **2** and **3** (15 mg, 0.025 mmol) was placed in a 20 mL vial equipped with a septum, and 10 mL of CO_2 (~0.45 mmol) were injected. The solution was vigorously stirred for a few seconds until a white precipitate was observed. The vial was introduced to the glovebox, 15 mL of pentane was added via syringe to the vial, and vacuum was applied for a few min to remove excess of CO_2. The precipitate was isolated by decantation and washed with 10 mL of pentane. Complex **6** was obtained as a white solid, and was dried under vacuum for only 30 min to avoid decomposition (~35% yield). Crystals of **6** suitable for X-ray analysis were obtained by layering a concentrated methyelen chloride or an acetone solution of **6** with pentane in an NMR tube at −30 °C. According to $^{31}P\{^{1}H\}$ NMR, complex **6** could not be obtained exclusively, but as the major product (70% by integration) in a mixture with an unidentified intermediate at 62 ppm and unidentified impurity at 42 ppm (see Supporting Information). The same mixture (with variation in the integration ratio of the signals) was obtained when crystals of **6** were redissolved in methylene chloride or acetone. The same mixture was obtained when the white precipitate was obtained upon addition of CO_2 to complexes **2** and **3**, without further addition of pentane.

Complex **6** decomposes in methylene chloride or acetone at ambient temperature to give a mixture of several unidentified complexes (see Supporting Information).

Complex **6** is not stable under vacuum. After 8 h under vacuum, the resulted solid was soluble in THF, and according to $^{31}P\{^{1}H\}$ NMR, the major product is complex **4** (65% yield by integration) (see Supporting Information).

Partial NMR characterization of **6** was possible *in situ*, with the aid of 2D NMR techniques.

$^{31}P\{^{1}H\}$ NMR (121 MHz, acetone-d_6, 298 K) δ: 52.11 (s).

^{1}H NMR (500 MHz, methylene chloride-d_2, 243 K) δ: −22.20 (t, 1H, $^{2}J_{PH}$ = 13.9 Hz, $^{2}J_{CH}$ = 3.8 Hz (observed when $^{13}CO_2$ was used), Ir-H), 1.25 (overlapping with residual signals of pentane, detected by P−H correlation experiment, P−C(CH_3)$_3$)), AB system centered at 3.47 and 3.74 (br d, 4H, $^{2}J_{HH}$ = 16.9 Hz, P-CH_2), 7.35 (d, 2H, $^{3}J_{HH}$ = 7.6 Hz, Py-CH), 7.69 (t, 1H, $^{3}J_{HH}$ = 7.6 Hz, Py-CH). $^{13}C\{^{1}H\}$ NMR (101 MHz, methylene chloride-d_2, 243 K) δ: 28.80 (br s, P−C(CH_3)$_3$), 28.88 (br s, P−C(CH_3)$_3$), 35.89 (vt, J_{PC} = 13.2 Hz, P-C(CH$_3$)$_3$), 36.97 (vt, J_{PC} = 10.1 Hz, P-C(CH$_3$)$_3$), 38.46 (vt, J_{PC} = 11.2 Hz, P-CH_2), 120.39 (vt, J_{PC} = 4.1 Hz, Py-CH), 128.35 (s, Py-CH), 138.22 (s, Py-CH), 161.17 (s, Ir−O-CO), 162.57 (vt, J_{PC} = 3.0 Hz, Py-C), 169.2 (br t, $^{2}J_{PC}$ = 7 Hz, Ir-CO). IR (of the isolated precipitate) (ν_{CO2}): 1705.8, 1664.6, and 1284.5 cm^{-1}; (of the isolated precipitate using $^{13}CO_2$): 1662.6, 1610.1, and 1260.7 cm^{-1}.

X-ray Structural Analysis of 6, Crystallization from Methylene Chloride–Pentane. Crystal Data: $C_{25}H_{44}IrNO_4P_2$ + $3CH_2Cl_2$, colorless plate, 0.278 × 0.209 × 0.101 mm^3, Monoclinic $P2_1/c$, a = 16.6996(4) Å, b = 15.2679(3) Å, c = 16.3378(4) Å, β = 116.667(3)°, from 58 988 reflections, T = 100(2)K, V = 3722.49(17) Å^3, Z = 4, Fw = 931.53, Dc = 1.662 mg·m^{-3}, μ = 4.136 mm^{-1}.

Data Collection and Processing. Rigaku XtalabPro equipped with Pilatus 200 K diffractometer, Mo Kα (λ = 0.71073 Å), $-20 \le h \le 20$, $-19 \le k \le 19$, $-20 \le l \le 19$, frame scan width = 0.5°, scan speed 1.0° per 20 s, 58 988 reflections collected, 7603 independent reflections (R_{int} = 0.0561). The data were processed with CrysAlis.

Solution and Refinement. Structure solved with SHELXT. Full matrix least-squares refinement based on F^2 with SHELXL on 412 parameters with no restraints gave final R_1 = 0.0233 (based on F2) for data with $I > 2\sigma(I)$ and, R_1 = 0.0272 on 7603 reflections, goodness-of-

DOI: 10.1021/jacs.6b00202
J. Am. Chem. Soc. 2016, 138, 6445–6454

fit on F^2 = 1.075, largest electron density peak 1.658 e·Å^{-3}. Largest hole, −0.823 e·Å^{-3}.

X-ray Structural Analysis of ***6****, Crystallization from Acetone–Pentane.* Crystal Data: $C_{25}H_{44}IrNO_4P_2$ + C_3H_6O, colorless prism, 0.269 × 0.090 × 0.060 mm^3, Orthorhombic $P2_12_12_1$, a = 12.2328(3) Å, b = 15.8577(4) Å, c = 16.0723(4) Å, from 29 064 reflections, T = 100(2)K, V = 3117.78(14) Å^3, Z = 4, Fw = 734.83, Dc = 1.565 mg·m^{-3}, μ = 4.420 mm^{-1}.

Data Collection and Processing. Rigaku XtalabPro equipped with Pilatus 200 K diffractometer, Mo Kα (λ = 0.71073 Å), $-15 \le h \le 15$, $-19 \le k \le 20$, $-20 \le l \le 20$, frame scan width = 0.5°, scan speed 1.0° per 20 s, 29 046 reflections collected, 7110 independent reflections (R_{int} = 0.0538). The data were processed with CrysAlis.

Solution and Refinement. Structure solved with SHELXT. Full matrix least-squares refinement based on F^2 with SHELXL on 333 parameters with no restraints gave final R_1 = 0.0252 (based on F^2) for data with $I > 2\sigma(I)$ and R_1 = 0.0296 on 7104 reflections, goodness-of-fit on F^2 = 0.949, largest electron density peak 1.905 e·Å^{-3}. Largest hole −0.953 e·Å^{-3}.

Computational Methods. All geometries were optimized with the BP86 generalized-gradient approximation (GGA) functional and the def2-SV(P) basis set together with corresponding core potential for ruthenium.[44] The D3 dispersion correction was used for the geometry optimizations.[45] This level of theory was also used for the population analysis. Thermodynamic properties were obtained at the same level of theory from a frequency calculation. Previous studies revealed that taking infinitely separated reactants as reference states leads to an overestimation of the entropy loss in bimolecular reactions, mainly because the loss of translational degrees of freedom is overestimated.[46] We therefore decided to take only the vibrational and rotational degrees of freedom into account when estimating the free energy changes. This is denoted in the manuscript as $\Delta G_{vib+rot}$. All free energies are calculated under standard conditions unless otherwise noted. Minima and transition states were characterized by the absence and presence of one imaginary frequency, respectively. Single point energies were obtained with the spin-scaled double hybrid functional DSD-PBEB86 with the D3 dispersion correction and Becke-Johnson dumping and the larger triple-ζ def2-TZVP basis set.[46c,47,47] The DSD-PBEB86-D3BJ functional was recently shown to yield results very close to explicitly correlated coupled cluster benchmark calculations for reaction energies and barriers involving transition metal complexes with pincer ligands.[48] To improve the computational efficiency, the density fitting approximation with the W06 fitting basis sets, designed for use with the def2 basis sets, was used for the BP86 calculations and the RIJCOSX with the appropriate def2-TZVP/J and def2-TZVP/C basis sets for the DSD-PBEB86 calculations.[49] To take solvent effects into account, the SMD solvation model for THF was used for the single point calculations.[50] The "ultrafine" (i.e., a pruned (99 590)) grid was used for the geometry optimizations and the "Finalgrid6" (i.e., a Lebedev 590 points grid) for the single point calculations. BP86 calculations were performed using Gaussian 09 Revision D.01.[51] The DSD-PBEB86-D3BJ calculations were performed with the ORCA program package.[52]

■ ASSOCIATED CONTENT

Supporting Information

The Supporting Information is available free of charge on the ACS Publications website at DOI: 10.1021/jacs.6b00202.

Experimental, spectroscopic and computational details (PDF)

Crystallographic datas (CIF)

■ AUTHOR INFORMATION

Corresponding Authors

*moran.feller@weizmann.ac.il

*david.milstein@weizmann.ac.il

Notes

The authors declare no competing financial interest.

■ ACKNOWLEDGMENTS

We thank the Israel Science Foundation for financial support. D.M. holds the Israel Matz Professorial Chair of Organic Chemistry.

■ REFERENCES

(1) (a) Kondratenko, E. V.; Mul, G.; Baltrusaitis, J.; Larrazabal, G. O.; Perez-Ramirez, J. *Energy Environ. Sci.* **2013**, *6*, 3112. (b) Wang, W.-H.; Himeda, Y.; Muckerman, J. T.; Manbeck, G. F.; Fujita, E. *Chem. Rev.* **2015**, *115* (23), 12936. (c) Ampelli, C.; Perathoner, S.; Centi, G. *Philos. Trans. R. Soc., A* **2015**, *373*, 20140177. (d) Fan, T.; Chen, X.; Lin, Z. *Chem. Commun.* **2012**, *48*, 10808. (e) Liu, Q.; Wu, L.; Jackstell, R.; Beller, M. *Nat. Commun.* **2015**, *6*, 5933. (f) Alberico, E.; Nielsen, M. *Chem. Commun.* **2015**, *51*, 6714. (g) Cokoja, M.; Bruckmeier, C.; Rieger, B.; Herrmann, W. A.; Kühn, F. E. *Angew. Chem., Int. Ed.* **2011**, *50*, 8510.

(2) Fernández-Alvarez, F. J.; Iglesias, M.; Oro, L. A.; Polo, V. *ChemCatChem* **2013**, *5*, 3481.

(3) Hanna, T. A.; Baranger, A. M.; Bergman, R. G. *J. Am. Chem. Soc.* **1995**, *117*, 11363.

(4) (a) Chapman, A. M.; Haddow, M. F.; Wass, D. F. *J. Am. Chem. Soc.* **2011**, *133*, 18463. (b) Flynn, S. R.; Wass, D. F. *ACS Catal.* **2013**, *3*, 2574. (c) Dickie, D. A.; Kemp, R. A. *Organometallics* **2014**, *33*, 6511. (d) Courtemanche, M.-A.; Larouche, J.; Légaré, M.-A.; Bi, W.; Maron, L.; Fontaine, F.-G. *Organometallics* **2013**, *32*, 6804. (e) Xu, X.; Kehr, G.; Daniliuc, C. G.; Erker, G. *J. Am. Chem. Soc.* **2013**, *135*, 6465. (f) Sgro, M. J.; Stephan, D. W. *Chem. Commun.* **2013**, *49*, 2610. (g) Dickie, D. A.; Ulibarri-Sanchez Iii, R. P.; Jarman, P. J.; Kemp, R. A. *Polyhedron* **2013**, *58*, 92. (h) Sgro, M. J.; Stephan, D. W. *Angew. Chem., Int. Ed.* **2012**, *51*, 11343. (i) Normand, A. T.; Daniliuc, C. G.; Wibbeling, B.; Kehr, G.; Le Gendre, P.; Erker, G. *J. Am. Chem. Soc.* **2015**, *137*, 10796. (j) Xu, X.; Kehr, G.; Daniliuc, C. G.; Erker, G. *J. Am. Chem. Soc.* **2014**, *136*, 12431.

(5) Sieh, D.; Lacy, D. C.; Peters, J. C.; Kubiak, C. P. *Chem. - Eur. J.* **2015**, *21*, 8497.

(6) LeBlanc, F. A.; Berkefeld, A.; Piers, W. E.; Parvez, M. *Organometallics* **2012**, *31*, 810.

(7) Braunstein, P.; Matt, D.; Dusausoy, Y.; Fischer, J.; Mitschler, A.; Ricard, L. *J. Am. Chem. Soc.* **1981**, *103*, 5115.

(8) (a) Langer, J.; Imhof, W.; Fabra, M. J.; García-Orduña, P.; Görls, H.; Lahoz, F. J.; Oro, L. A.; Westerhausen, M. *Organometallics* **2010**, *29*, 1642. (b) Herskovitz, T.; Guggenberger, L. J. *J. Am. Chem. Soc.* **1976**, *98*, 1615.

(9) Dahlenburg, L.; Prengel, C. *J. Organomet. Chem.* **1986**, *308*, 63.

(10) (a) Paparo, A.; Silvia, J. S.; Kefalidis, C. E.; Spaniol, T. P.; Maron, L.; Okuda, J.; Cummins, C. C. *Angew. Chem., Int. Ed.* **2015**, *54*, 9115. (b) Andrez, J.; Pécaut, J.; Bayle, P.-A.; Mazzanti, M. *Angew. Chem., Int. Ed.* **2014**, *53*, 10448. (c) Evans, W. J.; Lorenz, S. E.; Ziller, J. W. *Inorg. Chem.* **2009**, *48*, 2001. (d) Evans, W. J.; Seibel, C. A.; Ziller, J. W. *Inorg. Chem.* **1998**, *37*, 770. (e) Angamuthu, R.; Byers, P.; Lutz, M.; Spek, A. L.; Bouwman, E. *Science* **2010**, *327*, 313. (f) Amatore, C.; Saveant, J. M. *J. Am. Chem. Soc.* **1981**, *103*, 5021.

(11) (a) Miyashita, A.; Yamamoto, A. *J. Organomet. Chem.* **1973**, *49*, C57. (b) Darensbourg, D. J.; Groetsch, G.; Wiegreffe, P.; Rheingold, A. L. *Inorg. Chem.* **1987**, *26*, 3827. (c) Johansson, R.; Jarenmark, M.; Wendt, O. F. *Organometallics* **2005**, *24*, 4500. (d) Schmeier, T. J.; Hazari, N.; Incarvito, C. D.; Raskatov, J. A. *Chem. Commun.* **2011**, *47*, 1824.

(12) Marsich, N.; Camus, A.; Nardin, G. *J. Organomet. Chem.* **1982**, *239*, 429.

(13) (a) Johansson, R.; Wendt, O. F. *Dalton Trans.* **2007**, 488. (b) Johnson, M. T.; Johansson, R.; Kondrashov, M. V.; Steyl, G.; Ahlquist, M. S. G.; Roodt, A.; Wendt, O. F. *Organometallics* **2010**, *29*, 3521.

DOI: 10.1021/jacs.6b00202
J. Am. Chem. Soc. 2016, 138, 6445−6454

(14) (a) Feller, M.; Ben-Ari, E.; Diskin-Posner, Y.; Carmieli, R.; Weiner, L.; Milstein, D. *J. Am. Chem. Soc.* **2015**, *137*, 4634. (b) Truscott, B. J.; Nelson, D. J.; Slawin, A. M. Z.; Nolan, S. P. *Chem. Commun.* **2014**, *50*, 286. (c) Lohr, T. L.; Piers, W. E.; Parvez, M. *Dalton Trans.* **2013**, *42*, 14742. (d) Huang, D.; Makhlynets, O. V.; Tan, L. L.; Lee, S. C.; Rybak-Akimova, E. V.; Holm, R. H. *Inorg. Chem.* **2011**, *50*, 10070. (e) Palmer, D. A.; Van Eldik, R. *Chem. Rev.* **1983**, *83*, 651. (f) Kitajima, N.; Hikichi, S.; Tanaka, M.; Morooka, Y. *J. Am. Chem. Soc.* **1993**, *115*, 5496. (g) Truscott, B. J.; Kruger, H.; Webb, P. B.; Bühl, M.; Nolan, S. P. *Chem. - Eur. J.* **2015**, *21*, 6930.

(15) (a) Newman, L. J.; Bergman, R. G. *J. Am. Chem. Soc.* **1985**, *107*, 5314. (b) Cui, D.; Nishiura, M.; Tardif, O.; Hou, Z. *Organometallics* **2008**, *27*, 2428.

(16) Rahim, M.; White, C.; Rheingold, A. L.; Ahmed, K. J. *Organometallics* **1993**, *12*, 2401.

(17) Park, A. *Bull. Korean Chem. Soc.* **2001**, *22*, 1410.

(18) McLoughlin, M. A.; Keder, N. L.; Harrison, W. T. A.; Flesher, R. J.; Mayer, H. A.; Kaska, W. C. *Inorg. Chem.* **1999**, *38*, 3223.

(19) (a) Kaska, W. C.; Nemeh, S.; Shirazi, A.; Potuznik, S. *Organometallics* **1988**, *7*, 13. (b) Leitner, W. *Angew. Chem., Int. Ed. Engl.* **1995**, *34*, 2207. (c) Scheuermann, M. L.; Semproni, S. P.; Pappas, I.; Chirik, P. J. *Inorg. Chem.* **2014**, *53*, 9463. (d) Vigalok, A.; Ben-David, Y.; Milstein, D. *Organometallics* **1996**, *15*, 1839. (e) Huang, K.-W.; Han, J. H.; Musgrave, C. B.; Fujita, E. *Organometallics* **2007**, *26*, 508.

(20) (a) Schmeier, T. J.; Dobereiner, G. E.; Crabtree, R. H.; Hazari, N. *J. Am. Chem. Soc.* **2011**, *133*, 9274. (b) Kang, P.; Cheng, C.; Chen, Z.; Schauer, C. K.; Meyer, T. J.; Brookhart, M. *J. Am. Chem. Soc.* **2012**, *134*, 5500. (c) Moret, S.; Dyson, P. J.; Laurenczy, G. *Nat. Commun.* **2014**, *5*, 4017. (d) Langer, R.; Diskin-Posner, Y.; Leitus, G.; Shimon, L. J. W.; Ben-David, Y.; Milstein, D. *Angew. Chem., Int. Ed.* **2011**, *50*, 9948. (e) Wang, W.; Wang, S.; Ma, X.; Gong, J. *Chem. Soc. Rev.* **2011**, *40*, 3703. (f) Jessop, P. G.; Joó, F.; Tai, C.-C. *Coord. Chem. Rev.* **2004**, *248*, 2425. (g) Federsel, C.; Boddien, A.; Jackstell, R.; Jennerjahn, R.; Dyson, P. J.; Scopelliti, R.; Laurenczy, G.; Beller, M. *Angew. Chem., Int. Ed.* **2010**, *49*, 9777. (h) Creutz, C.; Chou, M. H. *J. Am. Chem. Soc.* **2007**, *129*, 10108. (i) Filonenko, G. A.; Conley, M. P.; Copéret, C.; Lutz, M.; Hensen, E. J. M.; Pidko, E. A. *ACS Catal.* **2013**, *3*, 2522.

(21) (a) Tanaka, R.; Yamashita, M.; Nozaki, K. *J. Am. Chem. Soc.* **2009**, *131*, 14168. (b) Tanaka, R.; Yamashita, M.; Chung, L. W.; Morokuma, K.; Nozaki, K. *Organometallics* **2011**, *30*, 6742.

(22) (a) Tanaka, H.; Nagao, H.; Peng, S. M.; Tanaka, K. *Organometallics* **1992**, *11*, 1450. (b) DuBois, D. L.; Miedaner, A.; Haltiwanger, R. C. *J. Am. Chem. Soc.* **1991**, *113*, 8753. (c) Downard, A. J.; Bond, A. M.; Clayton, A. J.; Hanton, L. R.; McMorran, D. A. *Inorg. Chem.* **1996**, *35*, 7684. (d) Raebiger, J. W.; Turner, J. W.; Noll, B. C.; Curtis, C. J.; Miedaner, A.; Cox, B.; DuBois, D. L. *Organometallics* **2006**, *25*, 3345. (e) Smieja, J. M.; Kubiak, C. P. *Inorg. Chem.* **2010**, *49*, 9283. (f) Smieja, J. M.; Sampson, M. D.; Grice, K. A.; Benson, E. E.; Froehlich, J. D.; Kubiak, C. P. *Inorg. Chem.* **2013**, *52*, 2484. (g) Costentin, C.; Drouet, S.; Passard, G.; Robert, M.; Savéant, J.-M. *J. Am. Chem. Soc.* **2013**, *135*, 9023. (h) Garg, K.; Matsubara, Y.; Ertem, M. Z.; Lewandowska-Andralojc, A.; Sato, S.; Szalda, D. J.; Muckerman, J. T.; Fujita, E. *Angew. Chem., Int. Ed.* **2015**, *54*, 14128. (i) Sato, S.; Morikawa, T.; Kajino, T.; Ishitani, O. *Angew. Chem., Int. Ed.* **2013**, *52*, 988.

(23) (a) Kobayashi, K.; Tanaka, K. *Inorg. Chem.* **2015**, *54*, 5085. (b) Machan, C. W.; Chabolla, S. A.; Yin, J.; Gilson, M. K.; Tezcan, F. A.; Kubiak, C. P. *J. Am. Chem. Soc.* **2014**, *136*, 14598. (c) Fachinetti, G.; Floriani, C.; Chiesi-Villa, A.; Guastini, C. *J. Am. Chem. Soc.* **1979**, *101*, 1767. (d) Alvarez, R.; Carmona, E.; Poveda, M. L.; Sanchez-Delgado, R. *J. Am. Chem. Soc.* **1984**, *106*, 2731. (e) Lee, G. R.; Maher, J. M.; Cooper, N. J. *J. Am. Chem. Soc.* **1987**, *109*, 2956.

(24) (a) Noor, A.; Qayyum, S.; Bauer, T.; Schwarz, S.; Weber, B.; Kempe, R. *Chem. Commun.* **2014**, *50*, 13127. (b) Kilpatrick, A. F. R.; Cloke, F. G. N. *Chem. Commun.* **2014**, *50*, 2769. (c) Krogman, J. P.; Foxman, B. M.; Thomas, C. M. *J. Am. Chem. Soc.* **2011**, *133*, 14582.

(25) Rivada-Wheelaghan, O.; Dauth, A.; Leitus, G.; Diskin-Posner, Y.; Milstein, D. *Inorg. Chem.* **2015**, *54*, 4526.

(26) Vogt, M.; Gargir, M.; Iron, M. A.; Diskin-Posner, Y.; Ben-David, Y.; Milstein, D. *Chem. - Eur. J.* **2012**, *18*, 9194.

(27) Vogt, M.; Nerush, A.; Diskin-Posner, Y.; Ben-David, Y.; Milstein, D. *Chem. Sci.* **2014**, *5*, 2043.

(28) Huff, C. A.; Kampf, J. W.; Sanford, M. S. *Organometallics* **2012**, *31*, 4643.

(29) Chakraborty, S.; Blacque, O.; Berke, H. *Dalton Trans.* **2015**, *44*, 6560.

(30) Khusnutdinova, J. R.; Milstein, D. *Angew. Chem., Int. Ed.* **2015**, *54*, 12236.

(31) Ben-Ari, E.; Leitus, G.; Shimon, L. J. W.; Milstein, D. *J. Am. Chem. Soc.* **2006**, *128*, 15390.

(32) Schwartsburd, L.; Iron, M. A.; Konstantinovski, L.; Diskin-Posner, Y.; Leitus, G.; Shimon, L. J. W.; Milstein, D. *Organometallics* **2010**, *29*, 3817.

(33) Kloek, S. M.; Heinekey, D. M.; Goldberg, K. I. *Organometallics* **2006**, *25*, 3007.

(34) Danopoulos, A. A.; Pugh, D.; Wright, J. A. *Angew. Chem., Int. Ed.* **2008**, *47*, 9765.

(35) Millard, M. D.; Moore, C. E.; Rheingold, A. L.; Figueroa, J. S. *J. Am. Chem. Soc.* **2010**, *132*, 8921.

(36) The calculated energy difference of 3.9 kcal/mol between complexes **2** and **3** predicts a ratio of 1:725, respectively.

(37) Although complexes **2** and **3** could not be obtained exclusively, they were always reproducibly formed as the major products (80%, according to $^{31}P\{^{1}H\}$ NMR) along with unidentified impurities, as depicted in Figure 1. Complexes **2** and **3** were thermally unstable and a mixture of unidentified products was obtained upon heating (70 °C) a solution of **2** and **3** in different solvents.

(38) The added volume of CO_2 was calculated approximately, using the molar volume of ideal gases.

(39) The $^{31}P\{^{1}H\}$ NMR of complex **4** exhibits a minor impurity (1% by integration) at 40 ppm. See Supporting Information.

(40) According to $^{31}P\{^{1}H\}$ NMR, two unidentified intermediate signals at 59 and 55 ppm were also observed just after CO_2 addition, but their signals disappeared.

(41) (a) Kohl, S. W.; Weiner, L.; Schwartsburd, L.; Konstantinovski, L.; Shimon, L. J. W.; Ben-David, Y.; Iron, M. A.; Milstein, D. *Science* **2009**, *324*, 74. (b) Carrión, M. C.; Ruiz-Castañeda, M.; Espino, G.; Aliende, C.; Santos, L.; Rodríguez, A. M.; Manzano, B. R.; Jalón, F. A.; Lledós, A. *ACS Catal.* **2014**, *4*, 1040. (c) Kovács, G.; Lledós, A.; Ujaque, G. *Organometallics* **2010**, *29*, 3252. (d) Li, H.; Hall, M. B. *J. Am. Chem. Soc.* **2014**, *136*, 383. (e) Sandhya, K. S.; Suresh, C. H. *Organometallics* **2013**, *32*, 2926. (f) Wang, W.-H.; Muckerman, J. T.; Fujita, E.; Himeda, Y. *ACS Catal.* **2013**, *3*, 856. (g) Schneider, S.; Meiners, J.; Askevold, B. *Eur. J. Inorg. Chem.* **2012**, *2012*, 412. (h) Friedrich, A.; Drees, M.; Schmedt auf der Günne, J.; Schneider, S. *J. Am. Chem. Soc.* **2009**, *131*, 17552. (i) Iron, M. A.; Ben-Ari, E.; Cohen, R.; Milstein, D. *Dalton Trans.* **2009**, 9433.

(42) A formato complex as local minimum was located on the potential energy surface. However, its free energy with respect to **3** and free CO_2 is −5.9 kcal/mol; therefore, this intermediate is 5.3 kcal/mol higher in energy than the intermediate **7*cis*** and 4 kcal/mol higher than **7*trans***. Our attempts to locate a transition state leading to the formato complex (based on carefully performed relaxed potential energy surface scans) resulted in dissociation to complex **3** and free CO_2. See Supporting Information.

(43) Fulmer, G. R.; Miller, A. J. M.; Sherden, N. H.; Gottlieb, H. E.; Nudelman, A.; Stoltz, B. M.; Bercaw, J. E.; Goldberg, K. I. *Organometallics* **2010**, *29*, 2176.

(44) (a) Becke, A. D. *Phys. Rev. A: At., Mol., Opt. Phys.* **1988**, *38*, 3098. (b) Perdew, J. P. *Phys. Rev. B: Condens. Matter Mater. Phys.* **1986**, *33*, 8822. (c) Weigend, F.; Ahlrichs, R. *Phys. Chem. Chem. Phys.* **2005**, *7*, 3297. (d) Dolg, M. In *Modern Methods and Algorithms of Quantum Chemistry*; Grotendorst, J., Ed.; John von Neumann Institute for Computing: Julich, 2000; Vol. 3, p 507.

(45) Grimme, S.; Antony, J.; Ehrlich, S.; Krieg, H. J. *J. Chem. Phys.* **2010**, *132*, 154104.

DOI: 10.1021/jacs.6b00202
J. Am. Chem. Soc. 2016, 138, 6445−6454

(46) Mondal, B.; Neese, F.; Ye, S. *Inorg. Chem.* **2015**, *54*, 7192−7198 and the literature cited therein.
(47) (a) Kozuch, S.; Martin, J. M. L. *Phys. Chem. Chem. Phys.* **2011**, *13*, 20104. (b) Johnson, E. R.; Becke, A. D. *J. Chem. Phys.* **2006**, *124*, 174104.
(48) Kesharwani, M. K.; Martin, J. M. L. *Theor. Chem. Acc.* **2014**, *133*, 1452.
(49) (a) Dunlap, B. I. *J. Chem. Phys.* **1983**, *78*, 3140. (b) Dunlap, B. I. *J. Mol. Struct.: THEOCHEM* **2000**, *529*, 37. (c) Weigend, F. *Phys. Chem. Chem. Phys.* **2006**, *8*, 1057. (d) Kossmann, S.; Neese, F. J. *Chem. Theory Comput.* **2010**, *6*, 2325. (e) Weigend, F.; Häser, M.; Patzelt, H.; Ahlrichs, R. *Chem. Phys. Lett.* **1998**, *294*, 143.
(50) Marenich, A. V.; Cramer, C. J.; Truhlar, D. G. J. *J. Phys. Chem. B* **2009**, *113*, 6378.
(51) Frisch, M. J.; Trucks, G. W.; Schlegel, H. B.; Scuseria, G. E.; Robb, M. A.; Cheeseman, J. R.; Scalmani, G.; Barone, V.; Mennucci, B.; Petersson, G. A.; Nakatsuji, H.; Caricato, M.; Li, X.; Hratchian, H. P.; Izmaylov, A. F.; Bloino, J.; Zheng, G.; Sonnenberg, J. L.; Hada, M.; Ehara, M.; Toyota, K.; Fukuda, R.; Hasegawa, J.; Ishida, M.; Nakajima, T.; Honda, Y.; Kitao, O.; Nakai, H.; Vreven, T.; Montgomery, J. A., Jr.; Peralta, J. E.; Ogliaro, F.; Bearpark, M.; Heyd, J. J.; Brothers, E.; Kudin, K. N.; Staroverov, V. N.; Keith, T.; R *Gaussian 09*, Revision D.01; Gaussian, Inc.: Wallingford, CT, 2009.
(52) Neese, F. *Comput. Mol. Sci.* **2012**, *2*, 73.

DOI: 10.1021/jacs.6b00202
J. Am. Chem. Soc. 2016, 138, 6445−6454